

Manuscript of the article: Sándor Szalai, Kitti Szokoli, Mohamed Metwaly, Delineation of landslide endangered areas and mapping their fracture systems by the pressure probe method. Appeared in: Landslides, 2014, Volume 11, Issue 5, pp. 923-932., doi: 10.1007/s10346-014-0509-6, ISSN: 1612-510X.

The final publication is available at [link.springer.com](http://link.springer.com):

<http://link.springer.com/article/10.1007%2Fs10346-014-0509-6>

## Delineation of Landslide Endangered Areas and Mapping their Fracture Systems by the Pressure Probe method

Sándor Szalai<sup>1</sup>, Kitti Szokoli<sup>1</sup>, Mohamed Metwaly<sup>2,3</sup>

1. MTA CSFK GGI, H-9401 Sopron POB 5, Hungary, e-mail: [szalai@ggki.hu](mailto:szalai@ggki.hu)
2. Archaeology Department, College of Tourism and Archaeology, King Saud University, Saudi Arabia.
3. National Research Institute of Astronomy and Geophysics (NRIAG), Cairo, Egypt.

Corresponding author: Sándor Szalai

RCAES HAS, GGI

H-9401 Sopron POB 5, Hungary, tel: 0036 99 508344, fax: 0036 99 508355,

e-mail: [szalai@ggki.hu](mailto:szalai@ggki.hu)

### Abstract

A new method, the so-called Pressure Probe (Pre-P) method has been developed for detecting and characterizing mechanically weak zones which may not be visible from the surface and which may occur e.g. due to landslides. On a high bank at Dunaszekcső, Hungary, the fracture system of the loess landslide area was investigated by large resolution applying this method and proved that: 1. cracks as small as 2-3 cm wide are detectable; 2. The fractures follow each other almost periodically; 3. On the side of the fractures towards the slump there are less fractured zones whose width correlates with the width of the given fracture. We also demonstrated that on the passive side of the clearly visible fracture: 1. There are also fractures along which future rock displacement is expected; 2. These fractures are at least as wide as the active side fractures; 3. The blocks there are about twice as wide as those on the active side. A block several meters wide is expected to fall before the main mass movement. The Pre-P method seems to be the most powerful tool to map the fracture system of such landslides because of its speed, simplicity of application, cost and interpretation. The Pre-P profiles and maps of the fracture system of a landslide enable to understand landslide evolution and delineate endangered areas earlier than by other methods.

**Keywords:** pressure probe method, delineation of landslides, fracture system, loess

### Introduction

Landslides are an increasing danger to human life and constructions with the increasing population and climate changes which induces heavy rains. It is therefore important to map landslide endangered areas, diagnose their risk and monitor them. To fulfil these requirements, the geophysical methods can be very useful. These techniques are summarised e.g. by Bogoslovsky and Ogilvy (1977), McCann and Forster, (1990) or Jongmans and Garambois (2007). Landslides and rockfalls can be investigated using seismic (e.g. Bichler et al, 2004, Walter et al. 2012), electrical (pl. Wisen et al 2003), electromagnetic (e.g. Méric et al, 2005) and GPR (pl. Bichler et al, 2004) methods. Combined use of different geophysical methods is common to improve their productivity, e.g. Bruno and Marillier (1999). The goal of the geophysical techniques used to be almost exclusively the horizontal and/or vertical delineation of the sliding mass. The inner structure of the landslide or the characterisation of the eventually existing sliding surface was studied less often.

Geotechnical methods like Core Sampling, Rotary Pressure Sounding (RPS), Cone Penetration Test Undrained (CPTU), Total Sounding (TS), Rotary Sounding, Vane Shear Tests and Pore Pressure Measurements (Solberg et al, 2012) are also very significant for studying landslides. CPTU is used to get information on sediment stratification and soil type. RPS is often used to detect quick clay and TS may be used to verify the depth to bedrock. Laboratory tests on material from core samples give detailed information on sediment stratification, soil type, shear strength, deformation properties, and permeability, etc. The engineering geological investigation of a slow moving landslide is presented in Sarah and M. R. Daryono (2012). Detailed descriptions of the geotechnical methods can be found in Gregersen and Løken (1983). Solberg et al. (2012) combined the geophysical and geotechnical approaches.

Remote sensing techniques are also very valuable tools in landslide investigations. Mapping the surface area affected by landslide is often done by observation of aerial photographs or remote sensing images (Van Westen, 2004) which indicate the topographical expression of the landslide. However, if the landslide is ancient or inactive, its morphologic features and boundaries may have been degraded by erosion and surface observations and measurements have to be supported by reconnaissance at depth (Dikau et al., 1996). The remote sensing techniques like Stereoscopic imagery, Satellite imagery and RADAR imagery used in the

1 detection and classification are collected in: ([http://geosun.sjsu.edu/paula/285/285/eb\\_sem.htm](http://geosun.sjsu.edu/paula/285/285/eb_sem.htm)). Remote sensing  
2 techniques are very useful in monitoring the movement of a landslide. The following methods can be used for  
3 this purpose: Global Positioning System (GPS), Satellite imagery, RADAR imagery, Stereophotogrammetry,  
4 Soft copy photogrammetry. A summary of the remote sensing techniques used to study landslides is given by  
5 Tofani et al (2013).

6 Geodetical methods are also distributed in landslide investigations as show by Újvári et al. (2009),  
7 Bányai et al. (2012), Bányai et al. (2013a) and Bányai et al. (2013b). Observation of landslides using GPS has  
8 become a firmly established technique over the past decade (e.g. Fukuoka et al., 1995; Jackson et al., 1996; Gili  
9 et al., 2000; Malet et al., 2002). Often it is applied together with deformation measurements, incorporating  
10 tiltmeters, inclinometers and extensometers (Cencetti et al., 2000; Coe et al., 2003; Corsini et al., 2005).

11 A physical modelling technique was applied to investigate the start and evolution of large scale  
12 landslides by Bachmann et al. (2004).

13 All of these techniques were mostly used in the investigation of landslides where the moving material  
14 differed from the remaining material. In our case the slump arose in a homogeneous rock mass. The physical  
15 properties of the area endangered by landslides are not different from the stable area so it cannot be delineated by  
16 geophysical tools. In this case the description of the sliding surface may still be useful because it determines the  
17 area which is going to move. Independent of the existence of any sliding surface, it is also possible to describe  
18 the fracture system which enables the delineation of the endangered area. If the fractures are visible on the  
19 surface, they can directly help in the delineation. However if they are not observable, they have to be detected  
20 using geodetic, geotechnical or geophysical methods. Geophysics has not been effective in this case but if the  
21 characteristic distance of the fractures were much larger, (about 10 m), Electric Resistivity Tomography was able  
22 to detect fractures (Francese et al 2009). The other possibility is to use geoelectric null-arrays (Szalai, Szarka,  
23 2008; Falco *et al.*, 2013). Geoelectric arrays can also be useful in determining fracture directions (Taylor and  
24 Fleming, 1988), but within strict limits (Szalai *et al.*, 2009).

25 Barnhardt and Kayen (2000) detected fractures by GPR, but the resolution of their measurements was  
26 only 5m and the results are questionable. The investigations by Jeannin et al. (2006) had very good resolution at  
27 the same time but they were carried out on a quarry wall, because the plateau above the cliff is covered with a  
28 conductive weathered layer, which drastically decrease the penetration depth of the GPR method.

29 The geotechnical tools which are theoretically useful in mapping fractures are expensive and their use is  
30 strongly limited by field conditions, like topography, artificial constructions, mass movement danger and  
31 vegetation, which limit or prevent access by vehicles which are necessary to carry out such measurements.

32 For these reasons we decided to use a method which avoids such problems and is fast, cheap and  
33 effective. The Pre-P method is just a simplified version of the CPT technique. The Pre-P method measures only  
34 the mechanical resistivity of the soil at shallow depths. This method is well applicable because most of the  
35 fractures reach close to the surface but they are not visible due to the vegetation cover and the soil eroded into  
36 them and fixed by roots. When crossing the roots of plants, the Pre-P instrument is able to detect fractures due to  
37 their decreased mechanical resistance. The investigation which was carried out using this principle will be  
38 presented later in more detail. As a result, it is possible to map the fracture system of the study area making  
39 possible the delineation of the endangered area in time.

## 40 **Geological and geomorphological settings**

41  
42 The study area belongs to the Baranya Hills (Fig. 1a). The monitored bank of the Danube stretches  
43 between the Sárköz and Mohács depressions for about 15 km (Moyzes and Scheuer, 1978) (Fig. 1b). These  
44 depressions were formed due to a tectonic movement along the main NE–SW and NW–SE structural lines  
45 during Quaternary, which also determined the present-day flow direction of the Danube (Moyzes and Scheuer,  
46 1978; Síkhgyi, 2002). Geophysical measurements support the idea that recent tectonic movements play a role in  
47 the evolution of the western bank of the Danube near Dunaszekcső, as they did in the past (Erdélyi, 1967). Using  
48 seismic tomography and reflection, Hegedűs et al. (2008) found an about W–E directed low-velocity tectonic  
49 zone below the northern edge of the slope failure at Dunaszekcső.

50 The basement formations at Dunaszekcső are Triassic–Jurassic limestones are located at 200–250 m  
51 below the surface (Szederkényi, 1964; Urbancsek, 1977; Moyzes and Scheuer, 1978; Hegedűs et al., 2008).  
52 These basement rocks are covered by clayey and sandy sediments formed in the Pannonian s.l. epoch (equivalent  
53 to the Upper Miocene and the Pliocene, 12.6 to ~2.6–2.4 Ma; Rónai, 1985) that can be found below about 70m  
54 depth under the southern moving block (SB) according to borehole data (Moyzes and Scheuer, 1978; Pécsi and  
55 Sheuer, 1979). The uppermost 70m of the sediment sequence at SB are sandy and clayey loess layers with brown  
56 to red fossil soils accumulated during the Pleistocene (Fig. 3). The bluff reaches its highest point (142 m a.s.l.) at  
57 Vár Hill where the southern part of the moving blocks is located (Fig 3). The flood plain of the Danube is very  
58 narrow or missing below SB at Vár Hill and the northern moving block (NB) at Szent János Hill. The bluff  
59 consists of a 20–30 m high vertical loess wall above the 10–20 m high slopes that consist of reworked loess from  
60

1 past landslides and fluvial mud, sand and gravel deposits of the Danube (Fig. 3). The slopes were intensively  
2 undercut by the river during each flood event (Moyzes and Scheuer, 1978; Kraft, 2005). The younger loess series  
3 on top is prone to collapse, while the older loess below is much more compact (Moyzes and Scheuer, 1978;  
4 Scheuer, 1979). The density of the younger loess deposits is around  $1.6\text{gcm}^{-3}$ , but that of the older loess series  
5 and the intercalated paleosols is between  $2.0\text{--}2.1\text{gcm}^{-3}$ , and that of the Pannonian clays and sands reaches  
6  $2.16\text{gcm}^{-3}$  (Hegedűs, et al., 2008). The ground water recharged from percolated rainfall and the Lánka stream  
7 resides in the lower part of the young and more porous loess deposits (Fig. 3). Ground water flows to the SE  
8 during base flow because of the sucking effect of the Danube (Moyzes and Scheuer, 1978).

9 Field observations show the development of tension cracks in the loess complex parallel as well as  
10 perpendicular to the channel of the Danube, indicating reduced rock strength. The vertical cracks are clearly  
11 visible on the roof of the Töröklyuk cave, a unique large natural cavity on NB. Cracking was probably induced  
12 by both previous sliding events and recent slumping. Recent tectonic movements may have also influenced this  
13 process because tension cracks have also appeared in the apparently intact part of the slope 150–200 m  
14 southwards from SB.

15 In addition, there are also hollows of various sizes on rock walls resulting from loess corrosion and  
16 piping (Kraft, 2005). This process could be activated anytime to open major cracks, as happened during the  
17 movements of the studied landslide. Landslides in the studied hill region are concentrated in areas where relative  
18 relief is sufficiently high. This situation occurs along the Danube bank where stream undercutting has produced  
19 relatively high bluffs. One of the most important factors of landsliding is the hydrological condition of high  
20 bluffs. The Danube has a water level fluctuation in a range of nearly 10 m that influences the springs of ground  
21 and artesian water at the foot of the bank, which is inundated during higher water stages but experiences rapid  
22 draining during lower water stages (Fábián et al., 2006).

23 Along the steep bank of the Danube, the Upper Pannonian sediment sequence consisting of alternating  
24 permeable and impervious layers is exposed in some places below the Pleistocene or Upper Pliocene loess  
25 sequence or the Pliocene red clays. Because of previous slumping and lateral erosion by the Danube, the Upper  
26 Pannonian sediments are partly redeposited with a disturbed stratification or buried under younger deposits. The  
27 Upper Pannonian sand deposits provide confined aquifers, and their water under pressure locally moistens the  
28 overlying past slump deposits, favouring the reactivation of existing slumps and the generation of new  
29 landslides. During spring–summer floods, the river inundates the surface to the level of the springs at the base of  
30 the bluff, leading to the rise of the local groundwater table. This circumstance is noteworthy because slumps and  
31 earthslides tend to take place after prolonged high-water stages of the Danube (Domján, 1952; Karácsonyi and  
32 Scheuer, 1972; Horváth and Scheuer, 1976; Pécsi et al., 1979; Fábián et al., 2006). According to the  
33 classification of Cruden and Varnes (1996), the past landslides at Dunaszekcső are historic landslide types,  
34 which developed under environmental conditions similar to today's. The numerous historic mass movements  
35 indicate the high landslide susceptibility of this area.

### 36 **Former researches in the area**

37  
38 Several regions of Hungary in the eastern part of Central Europe are susceptible to landslides among  
39 which the bluff along the west bank of the River Danube between Budapest and Mohács is the most affected  
40 (Fig. 1a; Farkas, 1983; Kleb and Schweitzer, 2001; Szabó, 2003). Mass movements have appeared on this part of  
41 the riverbank since the Roman times (Lóczy et al., 1989; Juhász, 1999). Based on the database of the Mining and  
42 Geological Bureau of Hungary more than 20 large landslides were recorded in the area during the 20th century  
43 (Fig. 1b). Recent major movements of the landslides have been studied from geomorphological (e.g. Bulla,  
44 1939; Pécsi, 1971; Pécsi et al., 1979), engineering geological (Egri and Párdányi, 1968; Kézdi, 1970; Karácsonyi  
45 and Scheuer 1972; Bendefy, 1972; Horváth and Scheuer, 1976; Scheuer, 1979; Pécsi and Scheuer, 1979), and  
46 hydrogeological (Domján, 1952; Galli, 1952; Schmidt Eligius, 1966) points of view. These studies mainly  
47 provided empirical descriptions of the 3D deformations. Geodetic measurements were carried out after a large  
48 slope failure at Dunaújváros in 1964 (Egri and Párdányi, 1968; Kézdi, 1970), but the results of these  
49 observations were only partially published (Kézdi, 1970). Consequently there is a lack of monitoring of  
50 landslides and their evolution in Hungary by means of both geodetic methods and modern tools (GPS, tiltmeters,  
51 etc.) in spite of current and potential problems in this region. In 2007, a large, about 220 m long rupture appeared  
52 parallel with the riverbank at Dunaszekcső (Figs. 1b and 2a,b). At that time the sliding mass was estimated at  
53 about  $0.3 \times 10^6 \text{ m}^3$  and its potential energy ( $U=mgh$ ) about 153.6 GJ, calculated with a centre of mass of 29 m  
54 elevation above the river. The landslide risk affected some properties and the river navigation. Thus, a GPS  
55 network complemented with borehole tiltmeters was established at this site to monitor movements and measure  
56 deformations. Strategies and implementation of GPS surveys vary with the type and size of movements and  
57 some other factors, e.g. the aim of monitoring and available resources. These measurements can be continuous in  
58 time (e.g. Mora et al., 2003, Puglisi et al., 2005) or discontinuous (e.g. Moss et al., 1999; Moss, 2000; Rizzo,  
59  
60  
61  
62  
63  
64  
65

2002; Squarzoni et al., 2005). The network and measurement strategy was selected and designed based on previous investigations of Bányai (2003a, b) and the above-mentioned studies.

### **The Pressure-probe (Pre-P) method**

We used a simplified penetrometer shown in figure 5a; the sketch of the measurement is displayed in figure 5b. The fractures of the study area are often hidden by vegetation and soil (Fig 5c). The plants themselves can also be good indicators of fractures due to e.g. their different colours in the micro-valleys sometimes arising along fractures. However, other tools are often required to map fractures. Therefore the Pre-P method using the deeper penetration of the penetrometer at the locations of fractures proved to be one of the most useful tools for this aim.

Our tool is a metal rod on which a metal disc is fixed to increase its weight (Fig. 5a). One lets it fall down from a height of 1 m as perpendicular as possible (Fig. 5c). This height was marked on the clothes of the crew members to hold it throughout the measuring process. The maximum measurable penetration depth was 30 cm which proved to be perfect in the study area. The measuring instrument sank deeper only in very wide fractures. In such locations 30 cm was noted which made possible to present the values here without distorting the profiles/maps by extremely large values.

The metal disc also prevented the tool from falling into visible or hidden fractures. The detailed description of the Pre-P instrument is in Appendix A. The Pre-P instrument was constructed to penetrate to a wide interval of depths to get the most possible information under field conditions. The tool proved to be perfect for this aim. It generally sank between 7 and 15 cm and larger values occurred only at fractures. In the future similar measurements are planned to be done using a penetrometer to locate the measuring points more precisely. In this way measurements could be carried out with smaller sampling distances.

### **Execution of the measurement**

The measurements were carried out on parallel profiles to map the fracture system of the study area. The distance of the profiles was 2 m and the sampling distance was 10 cm. The direction of the profiles was quasi perpendicular to the supposed direction of the most interesting fractures which are nearly parallel to the edge of the hill. Generally only the penetration depth of the probe was recorded but if the value was remarkably different from the surrounding ones, the environment of the given point was investigated in more detail. It was done by thrusting a metal rod around the given position looking for mechanically weak zones. If zones were found which seemed to be connected to the one in the profile, the vegetation was removed by a metal rod. If a fracture was found there, it was followed for a distance (Fig 5d) by removing the vegetation along the fracture by hand and/or by a metal rod (Fig. 5d). Several fractures were found in this way (Fig. 5e) and many of them were excavated for longer distances (Fig. 5f).

The linear micro valleys also aided the detection of fractures. These areas and those with plants having a different colour were more carefully investigated. The combined use of these methods further improved the effectiveness of the Pre-P measurements and confirmed the results.

## **Results and interpretation**

### **Profiling**

The map of the study area with profiles N6-S20 is presented in figure 2. Before interpreting it, we are going to interpret several profiles individually.

Significant, wide fractures were interpreted where the Pre-P values were much larger than in the neighbouring points. Outstanding values sometimes occurred only at one single measuring point but more often at several neighbouring points (Figs. 6 and 7). Zones were assigned to all dominant fractures. These are the zones which are on their eastern side and elongate from the given dominant fracture to the next dominant one. These zones were delineated by continuous line rectangles and numbered (see Fig. 6). These main fracture zones were further divided into smaller zones which belong to moderately significant, thinner fractures. These sub-zones were delineated by dotted line rectangles. The background values (where there are no fractures) were characteristically under 13 cm, mostly in the range of 11-13cm. Higher values most likely refer to the presence of fractures. The narrow range of the background values verifies both the homogeneity of the loess and the robustness of the Pre-P method.

At first a few typical profiles are presented and interpreted. They were measured in the area which has already started to slump, that is eastward from the MF and which is directly visible. It is 20-80 cm wide and the vertical displacement along it is in the range of 10-70cm. Five prominent anomalies are clearly recognisable on profile N6 (Fig. 6a.). They are most likely linked to major cracks. There is only one much smaller crack of 0.3 m west of the MF at 3.6-4.2 m. It is easily recognisable producing a strong local anomaly.

1 East of the MF approaching to the edge, the cracks follow each other ever more frequently. It can also  
2 be seen that on both sides of the fractures there are mechanically consolidated, stable zones and that they are  
3 wider in the active, eastern side than in the passive, western one. Between the cracks the mechanical resistance  
4 of the soil seems to follow a nearly sinusoidal distribution (marked by a blue line). The wider a crack, the wider  
5 is the consolidated zone on its eastern side. One should mention that small Pre-P values (usually below 11 cm)  
6 observed in the left end of the profile, are due to vehicles. The situation is the same for most of our profiles  
7 because they started in the path compressed by vehicles.

8 Although profile N4 (Fig. 6b) is just two meters away from profile N6 - only three remarkable zones  
9 can be seen. The first two can be divided into numbers of sub-zones. The large anomaly at 16.7 m suggests a  
10 mass fall along the surface perpendicular to the profile before the main slump along the MF (around 8 m).

11 There are many small cracks on profile S6 (Fig. 7a), east of the MF at about 5 m. It can be clearly seen  
12 that fracture zones 2-5 east of MF are narrowing towards the Danube River. Thinner cracks (in the left sides of  
13 the dotted rectangles) are present every 1-2 meters. This distance is in very good correlation with those observed  
14 in the cave at Töröklyuk which is close to the measuring area (Újvári et al, 2009). This fracture density proved to  
15 be typical in the study area, especially below the S-labelled profiles. A rock fall can happen anytime on profile  
16 S6 at about 0.7 m.

17 On the southernmost profile of the area (S20, Fig. 7b), four fracture zones can be recognised. The  
18 stability of the first and especially that of the third zone where there are actually only minor cracks is interesting.  
19 There is a weekend house in this stable zone to the south, about 10 m from the profile. Its walls are not yet  
20 cracked, which supports our Pre-P results.

21 The above examples illustrate that with an appropriate sampling distance (which was 10 cm) the Pr-P  
22 method is able to detect and localise cracks (at least in areas similar to the one we investigated), as well as to  
23 estimate their width.

## 24 Mapping

25 The Pr-P map is presented in figure 8. Beside of the fractures observable on the surface and marked by  
26 continuous yellow lines, numerous other fractures are clearly interpreted from the map. Such fractures are  
27 marked by yellow or purple dotted lines according to whether their direction is quasi-parallel or perpendicular to  
28 the hill edge. The width of the lines correlates with the supposed width of the cracks. There are two nearly  
29 perpendicular (XI -XII) fractures in the active area 10, to the edge parallel (I-X). The delineation of the  
30 compacted zones where the soil has a high mechanical resistance (marked by Arabic numerals) played an  
31 important role in marking the cracks.

32 On the basis of this map, a rock fall is expected along cracks VII and VIII before slumping along the  
33 MF.

34 The nearly parallel fractures are about 1-1.5 m from each other near the edge (0-12 m on the  $x$  axis), and  
35 about 3-4 m farther from the edge (12-21 m on the  $x$  axis) with the exception of stable zones, especially area 3c.

36 Reinforcing the Pre-P results, some cracks were shorter or longer exposed which is discussed in section  
37 "The construction of measurement".

38 The longest fracture we explored is drawn by wide black dashed lines in figure 8. Although its trace  
39 coincides mainly with fracture II both in the southern and the northern part of the map, the trace diverged from it  
40 and merged into other supposed cracks. It is most likely due to transverse cracks which "diverted" the trace from  
41 the "principal" direction of the area. At the branching points only one crack was followed from all the possible  
42 fractures. Although fracture II is typically not wider than 5 cm, it is clearly shown on the map, showing the  
43 effectiveness of the Pr-P method. It was able to detect even much thinner cracks than the sampling distance. If  
44 the profiles were taken closer to each other, one could get an even better image of the fracture system.

45 Delineation of stable zones can strongly support drawing the cracks. These stable zones always appear  
46 on the active side of the fractures (Fig. 8) in both larger dimensions (e.g. 3a, b, c and d zones which belong to the  
47 MF), and also in smaller dimensions (e.g. zone 5 in front of fracture II).

48 In our measurements we focused on the cracks which are quasi-parallel to the wall since they are  
49 decisive in terms of slumping. This is why the measurements were carried out perpendicular to the wall.  
50 Therefore the sampling distance was much smaller in this direction than parallel to the wall. Cracks  
51 perpendicular to the wall could be mapped in more detail, using the appropriate measuring direction.

52 Overall assessment of the map provides the following conclusions: 1. The Pre-P method is appropriate  
53 to map the fracture system of an area; 2. In the area we studied, many cracks were observed almost parallel to the  
54 edge whose distance is around 1-2 m. The existence of several cracks was confirmed by exploring them. 3. Due  
55 to the sampling direction, cracks perpendicular to the wall could not have been detected in detail. 4. Along  
56 cracks No. VII and VIII, mass movement may happen anytime, even before the slumping along the MF. 5. In  
57 order to get a better image, profiles should be taken closer to each other. A 1 m offset seems to be a good  
58 compromise between the effectiveness of measurement and the required investment.

## Investigating of the area that is not yet endangered

The main objective of the present study was to prove whether the Pre-P method is suitable for mapping the fissure system of an area and also to delineate the landslide endangered areas. The delineation seemed impossible because most of the area beyond the MF was cultivated, which prevents the use of the Pre-P method. For this reason, measurements were performed only along two profiles, which proved to be very informative. The most likely reason is that the cultivation of this area finished a long time ago.

Figure 9 displays the running average each of 3 consecutive values measured on profile P1 (Fig. 2). (Such averaging enables simpler interpretation, but it can lead to information loss which has to be therefore controlled). It is clearly seen that the area, which is located on the stable, not-sliding, passive side (0-49 m) from the MF is also fractured. The cracks in this zone have greater amplitude than on the active side (49-72 m). The fragmentation of the loess appears to have been also started here. It is not surprising considering the dimensions of the Castle Hill: the height of the hill above the level of the Danube River is about 50 m while it is approximately 90 m long in the direction perpendicular to the riverbed (see Fig 3). It is worth mentioning that on the passive side of the MF there are 3 blocks, about 10 m wide (0-10 m, 23-34 m, 38-48 m). On the active side the blocks are only about 3-6 m wide. There are only two cases of penetration values below 13 cm: the anomaly at 43-45 m shows both wheel tracks which are definitely recognizable. The reason for the anomaly at about 21 m is unknown.

The active side of the profile is more fragmented as indicated by the higher density of thin cracks which is denoted by dashed arrows. Cracks are supposed to be where the Pre-P values exceed 15 cm. The selection of this threshold value is somewhat artificial but since the area is fairly homogeneous, the designation of such a specific value can be justified. If the area were more inhomogeneous, one would have to take the local anomalies into consideration. While in the active side of the MF there are 5+9 smaller and larger cracks within the 23 m length (MF is not taken into consideration), in the passive side there are 6+10 cracks 48 m in length. Thus while the average distance between the cracks is 1.5 m in the active side, it is 3 m on the passive side.

It is also important to note that it is although advisable to regard the running average representation for easier interpretation of the results (see e.g. Fig. 9) this form of presentation can lead to information loss. The original, not averaged values of the major anomalies are not smaller on the active side than on the passive one, so the width of the cracks must be about the same on both sides.

These profile measurements thus proved the following: 1. There are cracks also in the area not yet endangered; 2. They are at least as wide as the cracks on the active side; 3. The passive area can be divided into blocks about twice as wide as the active area; 4. There is lateral displacement already present in locations where it is expected ; 5. The inner structure of the blocks is also visible inside the passive area, proving the very fine resolution of the method in spite of the former agricultural activity.

The results of the other profile, which is partly in the passive area (P1, shown in Fig 10, where the cracks are indicated by green lines) confirm the following: 1. There are also cracks in the passive area; 2. The major ones of the passive area are nearly parallel to each other having about the same 10 m and 14-15 m distance from the MF on both the P1 and P2 profiles; 3. While the background Pre-P value is about 15 cm on profile P2, it is only 11 cm on profile P1. This means that the area below P1 is most likely more consolidated. 4. The anomalies of P1 are at least as large, which may nevertheless be an alert.

## Conclusions

A new, extremely easy to use method, the pressure probe technique was introduced which measures a parameter proportional to the mechanical resistance of the soil. This method makes it possible to map fissure systems and to delineate loose or tight zones in areas threatened by landslides. The method thus allows a better understanding of the evolution of landslides and their delineation in appropriate circumstances when other methods might not be able to do that.

The major advantages of the method are: 1. its low cost; 2. its relative rapidity; 3. its almost arbitrarily high resolution power; 4. its easy use; 5. easy interpretation of its results; and 6. it can be used in almost any field conditions. It can be used among any topographic conditions, even in areas inaccessible by vehicles due to vegetation or landslide risk.

The main limit of the method is that it cannot be applied in areas where the mechanical properties of the soil have been exposed to artificial changes, e.g. in agricultural areas, or in areas visited by vehicles. The method would also be applicable in such cases but the depth of penetration would have to be increased. Since it requires great mechanical strength, the use of engines it would lose most of benefits listed above.

In spite of the noise which evidently occurs, the Pre-P method may work correctly as shown in the example that is presented. When using this method to detect the fracture system of a landslide, it is essential that

the fractures reach close to the surface. Fortunately this is often the situation. The fractures are often not visible only due to vegetation cover or erosion.

If excavations are carried out simultaneously with the Pre-P field measurements at the positions where cracks are suspected, even cracks 2-3 cm wide can be explored and tracked. Increasing the sampling distance may lead to a loss detection of fractures, especially the thin ones. Thus, it is recommended to make the sampling distance no greater than three times the width of the expected crack. No other known methods can produce similar resolution images of the fracture system except for geotechnical ones which are, much more expensive than the Pre-P method.

The fracture system of our study area has been mapped using the Pre-P method and we concluded the following: 1. even the thinner fractures are detectable because the resolution of the measurement is very fine; 2. both the major and the minor fractures follow each other almost periodically; 3. a well consolidated zone is attached to the fractures on the side towards the edge of the hill; 4. the fractures are often interrupted or branch out.

The results obtained measuring in the passive area showed the following: 1. cracks are present there too; 2. the cracks here are at least as wide as the cracks in the active area; 3. the future rupture surfaces already exist; 4. in this area the blocks are about twice as wide as those in the active area.

The Pre-P enables the localisation of future rupture surfaces and the delineation of the endangered areas. In addition, it can be predicted that: 1. near the scarp a detachment may easily occur before the slump along the MF; 2. the southern part of the study area is less endangered than the northern one (the area where profile P1 is more stable than that of the area of profile P2).

The method worked well in the study area although a part of it had been cultivated.

The Pre-P method is particularly useful for examination of landslides consisting of homogeneous rocks whose investigation is fairly limited by other methods. It may also be applicable for studying landslides with more heterogeneous composition but in this case less significant results can be expected.

In this article it was demonstrated that this economic method is very useful in delineation of potential landslide hazardous areas and for mapping their fracture system if the study area is not heavily influenced by human activity.

## **Appendix A**

### **The measuring device**

The principle of the Pre-P method using a manual pressure probe is simple: When the probe is dropped from the same height, its penetration depth depends on mechanical resistance of the soil. The probe consists of two parts (Fig. 5a): the T-shaped metal rod and the discs superimposed on it to increase its weight. The probe weighs 2,790 g, and the rod itself is 390 g. Its total length is 50 cm; its maximum penetration depth is 30 cm. There is a depth scale on the rod.

The diameter of the metal rod is 10 mm; the diameter of the tip end is 1.8 mm. The diameter of the 20 mm thick lower weight is 140 mm. It prevents the probe from dropping into wider cracks. The smaller weight above is 56 mm in diameter, and it is 120 mm thick. This design facilitates the vertical drop reducing this type of error. The ideal drop height is 1 m, which is convenient for most people. However, if necessary, it is possible to drop the probe from a larger height to get reasonable results in more compact soils. In such cases, increasing the weight of the probe or using a penetrometer might be simpler.

## **Acknowledgement**

S. Szalai, one of the authors of this paper received a grant from the János Bolyai Scholarship. We would also like to express our thanks to Ádám Tóth and Csaba Molnár for their aide in the field surveys and data processing.

## **References**

- Bachmann D, Bouissou S, Chemenda A (2004) Influence of weathering and pre-existing large scale fractures on gravitational slope failure: insights from 3-D physical modelling. *Natural Hazards and Earth System Sciences* 4:711–717
- Bányai L (2003a) Geodynamic investigations along the Mecsek-fault in Hungary using precise geodetic devices. Dept. of Civil Engineering, Patras University, pp 65–70
- Bányai L (2003b) Stability investigations of the high bank of river Danube in the area of Dunaföldvár. Dept. of Civil Engineering, Patras University, pp 265–271



- 1 Bányai L, Újvári G, Mentés Gy (2012) Kinematics and dynamics of a river bank failure determined by integrated  
2 geodetic observations - Case study of Dunaszekcső Landslide, Hungary. Proceeding of the annual  
3 International Conference on Geological & Earth Sciences (GEOS 2012), ISSN 2251-3361. 36:51-54
- 4 Bányai L, Újvári G, Mentés Gy (2013a) A dunaszekcsői magaspártcsuszamlás geodéziai megfigyelése (in  
5 Hungarian). *Geodézia és Kartográfia* 2013-11-12, 65:7-11
- 6
- 7 Bányai L, Újvári G, Mentés Gy, Kovács M, Czap Z, Gribovszki K, Papp G (2013b) Recurrent landsliding of a  
8 high bank at Dunaszekcső, Hungary: geodetic deformation monitoring and finite element modeling.  
9 *Geomorphology*
- 10
- 11 Barnhardt WA, Kayen RE (2000) Radar Structure of Earthquake-Induced, Coastal Landslides in Anchorage,  
12 Alaska, *Environmental Geosciences* 7(1):38-45
- 13
- 14 Bendefy L (1972) A dunaföldvári partcsuszamlás (The Dunaföldvár landslide). *Földrajzi Közlemények* 20:1–17  
15 (in Hungarian)
- 16
- 17 Bichler A, Bobrowsky P, Best M, Douma M, Hunter J, Calvert T, Burns R (2004) Three-dimensional mapping  
18 of a landslide using a multi-geophysical approach: the Quesnel Forks landslide. *Landslides* 1:29-40
- 19
- 20 Bogoslovsky VA, Ogilvy AA (1977) Geophysical methods for the investigation of landslides. *Geophysics*  
21 42:562-571
- 22
- 23 Bruno F, Marillier F (1999) Test of high-resolution seismic reflection and other geophysical techniques on the  
24 boup landslide in the swiss alps, *Engineering Geology* 52:113–120
- 25
- 26 Bulla B (1939) Teraszvizsgálatok Budapest és Adony között (Investigations of terraces between Budapest and  
27 Adony). *Földrajzi Közlemények* 63:92–107 (in Hungarian)
- 28
- 29 Cencetti C, Conversini P, Radicioni F, Ribaldi C, Sellì S, Tacconi P (2000) The evolution of Montebestia  
30 landslide (Umbria, Central Italy). Site investigations, in-situ tests and GPS monitoring. *Physics and  
31 Chemistry of the Earth (B)* 25:799–808
- 32
- 33 Coe JA, Ellis WL, Godt JW, Savage WZ, Savage JE, Michael JA, Kibler JD, Powers PS, Lidke DJ, Debray S  
34 (2003) Seasonal movement of the Slumgullion landslide determined from Global Positioning System surveys  
35 and field instrumentation, July 1998–March 2002. *Engineering Geology* 68:67–101
- 36
- 37 Corsini A, Pasuto A, Soldati M, Zannoni A (2005) Field monitoring of the Corvara landslide (Dolomites, Italy)  
38 and its relevance for hazard assessment. *Geomorphology* 66:149–165
- 39
- 40 Cruden DM, Varnes DJ (1996) Landslide types and processes. In: Turner AK, Schuster RL (Eds.), *Landslides:  
41 Investigation and Mitigation*, Special Report, vol. 247. Transportation Research Board, National Research  
42 Council, National Academy Press, Washington, DC, pp 36–75
- 43
- 44 Dikau R, Brundsen D, Schrott L, Ibsen M-L (1996) *Landslide recognition: identification,  
45 movement and causes*. Wiley, Chichester, UK, 274 p.
- 46
- 47 Domján J (1952) Középdunai magaspártok csúszásai (Slides of the bluffs along the middle reach of the River  
48 Danube). *Hidrológiai Közlöny* 32:416–422 (in Hungarian)
- 49
- 50 Egri Gy, Párdányi J (1968) Dunaújvárosi magaspártok állékonyság vizsgálata (Stability investigations of the  
51 high banks at Dunaújváros). *Műszaki Tervezés* 7:19–24 (in Hungarian)
- 52
- 53 Erdélyi M (1967) A Duna-Tisza közének vízföldtana (Hydrogeology of the Danube-Tisza Interfluve).  
54 *Hidrológiai Közlöny* 47:331–340.
- 55
- 56 Fábrián SZÁ, Kovács J, Lóczy D, Schweitzer F, Varga G, Babák K, Lampért K, Nagy A (2006) Geomorphologic  
57 hazards in the Carpathian foreland, Tolna County (Hungary). *Studia Geomorphologica Carpatho-Balcanica*  
58 40:107–118.
- 59
- 60
- 61
- 62
- 63
- 64
- 65

- 1 Falco P, Negro F, Szalai S, Milnes E (2013) Fracture characterisation using geoelectric null-arrays, *Journal of Applied Geophysics* 93:33–42
- 2
- 3 Farkas J (1983) Agyagok réteghatárán bekövetkező felszínmozgások (Surface mass movements occurring along  
4 the boundaries of clay layers). *Mélyépítéstudományi Szemle* 8:355–361
- 5
- 6 Francese R, Mazzarini F, Bistacchi A, Morelli G, Pasquarè G, Praticelli N, Robain H, Wardell N, Zaja A (2009)  
7 A structural and geophysical approach to the study of fractured aquifers in the Scansano-Magliano in  
8 Toscana Ridge, southern Tuscany, Italy, *Hydrogeology Journal* 17:1233–1246
- 9
- 10 Fukuoka H, Kodama N, Sokobiki H, Sassa K (1995) GPS monitoring of landslide movement. *Proceedings of the*  
11 *International Sabo Symposium, Tokyo*
- 12
- 13 Galli L (1952) A dunai és balatoni magaspártok állékonyságának törvényszerűségei (The rules of the stability of  
14 high bluffs along the Danube and Lake Balaton). *Hidrológiai Közlöny* 32:409–415 (in Hungarian)
- 15
- 16 Gili JA, Corominas J, Rius J (2000) Using Global Positioning System techniques in landslide monitoring.  
17 *Engineering Geology* 55:167–192
- 18
- 19 Gregersen O, Løken T (1983) Mapping of quick clay landslide hazard in Norway. *Criteria and*  
20 *experiences. SGI Rep* 17:61–174
- 21
- 22 Hegedüs E, Kovács ACS, Fancsik T (2008) A megcsúszott dunaszekcsői löszfal aktív és passzív szeizmikus  
23 vizsgálata (Active and passive seismic investigation of the slipped loess bluff at Dunaszekcső).  
24 *Research Report of the Eötvös Loránd Geophysical Institute, 20 pp*
- 25
- 26 Horváth Zs, Scheuer Gy (1976) A dunaföldvári partrogyás mérnökgeológiai vizsgálata (Engineering geological  
27 investigation of the bank collapse at Dunaföldvár). *Földtani Közlöny* 106:425–440 (in Hungarian)
- 28
- 29 Jackson ME, Bodin PW, Savage WZ, Nel EM (1996) Measurement of local velocities on the Slumgullion  
30 landslide using the Global Positioning System. In: Varnes DJ, Savage WZ (Eds.), *The Slumgullion Earth*  
31 *Flow: A Large-Scale Natural Laboratory. U.S. Geological Survey Bulletin* 2130:93–95
- 32
- 33 Jeannin M, Garambois S, Jongmans DG (2006) Multiconfiguration GPR measurements for geometric fracture  
34 characterization in limestone cliffs (Alps), *Geophysics* 71(3):B85–B92
- 35
- 36 Jongmans D, Garambois S (2007) Geophysical Investigation of Landslides: a review, *Bulletin Société*  
37 *Géologique de France* 178(2):101-112.
- 38
- 39 Juhász Á (1999) A klimatikus hatások szerepe a magaspártok fejlődésében (Role of climatic effects in the  
40 development of high banks). *Földtani Kutatás XXXVI*, pp 14–20 (in Hungarian)
- 41
- 42 Karácsonyi S, Scheuer Gy (1972) A dunai magaspártok építésföldtani problémái (Engineering geological  
43 problems of high banks along the Danube). *Földtani Kutatás* 15:71–83 (in Hungarian)
- 44
- 45 Kézdi Á (1970) A dunaújvárosi partrogyás (The bank collapse at Dunaújváros). *Mélyépítéstudományi Szemle*  
46 *20:281–297 (in Hungarian)*
- 47
- 48 Kleb B, Schweitzer F (2001) A Duna csuszamlásveszélyes magaspártjainak településkörnyezeti hatásvizsgálata  
49 (Assessment of the impact of landslide prone high banks on urban environment along the River Danube). In:  
50 Ádám A., Meskó A. (Eds.), *Földtudományok és a földi folyamatok kockázati tényezői. Bp. MTA*, pp 169–  
51 193 (in Hungarian)
- 52
- 53 Kraft J (2005) A dunaszekcsői Töröklyuk kialakulása és fennmaradása (Evolution and survival of the Töröklyuk  
54 cave at Dunaszekcső). *Mecsek Egyesület Évkönyve a 2004-es egyesületi évről. Új Évfolyam* 8:133–153 (in  
55 Hungarian)
- 56
- 57 Lóczy D, Balogh J, Ringer Á (1989) Landslide hazard induced by river undercutting along the Danube. In:  
58 Embleton, C., Federici, P.R., Rodolfi, G. (Eds.), *Geomorphological Hazards, Supplements of Geografia*  
59 *Fisica e Dinamica Quaternaria* 2:5–11
- 60
- 61
- 62
- 63
- 64
- 65

- 1 Malet JP, Maquaire O, Calais E (2002) The use of Global Positioning System techniques for the continuous  
2 monitoring of landslides: application to the Super-Sauze earthflow (Alpes-de-Haute-Provence, France).  
3 *Geomorphology* 43:33–54
- 4  
5 McCann DM, Forster A (1990) Reconnaissance geophysical methods in landslide investigations, *Engineering*  
6 *Geology* 29:59–79
- 7  
8 Meric O, Garambois S, Jongmans D, Wathelet M, Chatelain JL, Vengeon JM (2005) Application of geophysical  
9 methods for the investigation of the large gravitational mass movement of Séchilienne, France. *Can.*  
10 *Geotech. J.* 42:1105–1115
- 11  
12 Mora P, Baldi P, Casula G, Fabris M, Ghirotti M, Mazzini E, Pesci A (2003) Global Positioning Systems and  
13 digital photogrammetry for the monitoring of mass movements: application to the Ca'di Malta landslide  
14 (northern Apennines, Italy). *Engineering Geology* 68:103–121
- 15  
16 Moss JL, McGuire WJ, Page D (1999) Ground deformation monitoring of a potential landslide at La Palma,  
17 Canary Islands. *Journal of Volcanology and Geothermal Research* 94:251–265
- 18  
19 Moss JL (2000) Using the Global Positioning System to monitor dynamic ground deformation networks on  
20 potentially active landslides. *International Journal of Applied Earth Observation and Geoinformation* 2:24–32
- 21  
22 Moyzes A, Scheuer Gy (1978) A dunaszekcsői magaspart mérnökgeológiai vizsgálata (Engineering geological  
23 investigation of the high bank at Dunaszekcső). *Földtani Közlöny* 108:213–226 (in Hungarian)
- 24  
25 Pécsi M (1971) Az 1970 évi dunaföldvári földcsuszamlás (The Dunaföldvár landslide in 1970). *Földrajzi*  
26 *Értesítő* 20:233–238 (in Hungarian)
- 27  
28 Pécsi M, Scheuer Gy (1979) Engineering geological problems of the Dunaújváros loess bluff. *Acta Geologica*  
29 *Hungarica* 22:345–353
- 30  
31 Pécsi M, Schweitzer F, Scheuer Gy (1979) Engineering geological and geomorphological investigations of  
32 landslides in the loess bluffs along the Danube in the Great Hungarian Plain. *Acta Geologica Hungarica*  
33 22:327–343
- 34  
35 Puglisi G, Bonaccorso A, Mattia M, Aloisi M, Bonforte A, Campisi O, Cantarero M, Falzone G, Puglisi B, Rossi  
36 M (2005) New integrated geodetic monitoring system at Stromboli volcano (Italy). *Engineering Geology*  
37 79:13–31
- 38  
39 Rizzo V (2002) GPS monitoring and new data on slope movements in the Maratea Valley (Potenza, Basilicata).  
40 *Physics and Chemistry of the Earth* 27:1535–1544
- 41  
42 Rónai A (1985) The Quaternary of the Great Hungarian Plain. In: Pécsi, M. (Ed.), *Loess and*  
43 *the Quaternary*. Akadémiai Kiadó, Budapest, 51–63
- 44  
45 Sarah D, Daryono MR (2012) Engineering Geological Investigation of Slow Moving Landslide in Jahiyang  
46 Village, Salawu, Tasikmalaya Regency, Indonesian *Journal of Geology* 7(1):27–38
- 47  
48 Scheuer Gy (1979) A dunai magaspartok mérnökgeológiai vizsgálata (Engineering geological investigation of  
49 the high banks of the Danube). *Földtani Közlöny* 109:230–254 (in Hungarian)
- 50  
51 Schmidt ER (1966) A dunaújvárosi 1964. évi partomlás (The landslip at Dunaújváros in 1964). *MÁFI Évi*  
52 *Jelentése 1964-ről* (Annual Report of the Geological Institute of Hungary from the year 1964)
- 53  
54 Síkhegyi F (2002) Active structural evolution of the western and central parts of the Pannonian basin: a  
55 geomorphological approach. *EGU Stephan Mueller Special Publication Series* 3:203–216
- 56  
57 Solberg IL, Hansen L, Ronning JS, Haugen ED, Dalsegg E, Tonnesen JF (2012) Combined geophysical and  
58 geotechnical approach to ground investigations and hazard zonation of a quick clay area, mid-Norway, *Bull*  
59 *Eng Geol Environ* 71:119–133
- 60  
61  
62  
63  
64  
65

- 1 Squarzonì C, Delacourt C, Allemand P (2005) Differential single-frequency GPS monitoring of the La Valette  
2 landslide (French Alps). *Engineering Geology* 79:215–229
- 3
- 4 Szabó J (2003) The relationship between landslide activity and weather: examples from Hungary. *Natural*  
5 *Hazards and Earth System Sciences* 3:43–52
- 6
- 7 Szalai S, Kósa I, Nagy T, Szarka L (2009): Effectivity enhancement of azimuthal geoelectric measurements in  
8 determination of multiple directions of subsurface fissures, on basis of analogue modelling experiments, 15th  
9 European Meeting of Environmental and Engineering Geophysics, Dublin, Ireland, 7 - 9 September 2009,  
10 Proceedings & Exhibitors' Catalogue Near Surface 2009, 25 pp
- 11
- 12 Szalai S, Szarka L (2008) On the classification of surface geoelectric arrays, *Geophysical Prospecting* 56:159–  
13 175
- 14
- 15 Szederkényi T (1964) A baranyai Duna menti mezozoós szigettrögök földtani viszonyai (Geological conditions  
16 of the Mesozoic blocks along the River Danube in county Baranya). *Földtani Közlöny* 94:27–32 (in  
17 Hungarian)
- 18
- 19 Taylor RW, Fleming AH (1988) Characterizing jointed systems by azimuthal resistivity surveys. *Ground Water*,  
20 26:464-474
- 21
- 22 Tofani V, Segoni S, Agostini A, Catani F, Casagli N (2013) Technical Note: Use of remote sensing for landslide  
23 studies in Europe, *Nat. Hazards Earth Syst. Sci.* 13:299–309
- 24
- 25 Újvári G, Mentés Gy, Bányai L, Kraft J, Gyimóthy A, Kovács J (2009) Evolution of a bank failure along the  
26 River Danube at Dunaszekcső, Hungary, *Geomorphology* 109:197–209
- 27
- 28 Urbancsek J (1977) Magyarország mélyfúrású kútjainak katasztere VII. Cadastre of the deep-drilling wells in  
29 Hungary VII, 268 pp
- 30
- 31 Van Westen CJ (2004) Geo-Information tools for landslide risk assessment: an overview of recent developments.  
32 In: Proc. 9th International. Symp. Landslides, Rio de Janeiro, Brazil, Balkema, Rotterdam, pp 39-56
- 33
- 34 Walter M, Schwaderer U, Joswig M (2012) Seismic monitoring of precursory fracture signals from a destructive  
35 rockfall in the Vorarlberg Alps, Austria, *Nat. Hazards Earth Syst. Sci.* 12:3545–3555
- 36
- 37 Wisen R, Christiansen AV, Auken E, Dahlin T (2003). Application of 2D laterally constrained inversion and 2D  
38 smooth inversion of CVES resistivity data in a slope stability investigation. In: Proc. 9th Meeting Env. Eng.  
39 Geophys., Prague, Czech Republic, EAGE Publications, Houten, The Netherlands, O-002
- 40

## 41 Figure Captures

42

43 **Fig. 1.** Landslide hazard in Hungary. a) Landslide endangered areas (after Farkas, 1983; Juhász, 1999 and Szabó,  
44 2003). 1. Zselic and Baranya–Tolna Hills; 2. Zala Hills; 3. high banks at Lake Balaton; 4. Visegrád Mountains  
45 and terraced region along the Danube; 5. high banks along the Danube; 6. North Hungarian Mountains and Hills;  
46 7. Zemplén Mountain and high banks along the River Hernád. Black coarse lines denote the high banks along the  
47 Lake Balaton, the River Danube and the River Hernád. b) Large landslides in the 20th century along the high  
48 bank of Danube between Budapest and Mohács (after Juhász, 1999; Kleb and Schweitzer, 2001). Locations and  
49 years of the landslides are shown. Black stars indicate local  
50 outcropping blocks of Triassic limestone; sl=structural line.

51

52

53 **Fig. 2.** Google image of the research area with the Pre-P profiles. Yellow solid line: main fracture. Yellow dotted  
54 line: Supposed major fractures outside of the active area on the basis of the P1 and P2 profiles. Blue curves: the  
55 actual scarps.

56

57 **Fig. 3.** Geological cross-section of the high bank at Dunaszekcső (after Moyzes and Scheuer, 1978; Pécsi et al.,  
58 1979; Kraft, 2005). Elevation and distance were derived from the digital terrain model which was provided by  
59 geodetic measurements of 433 points. Vertical exaggeration: ×3. GWL=ground water level (measured in a well  
60 in July 2008); HW=highest

water; LW=lowest water.

1  
2 **Fig. 4** a. The loess mass which has already slumped looking from the south, (the direction of the study area.) b.  
3 The quasi vertical scarp. The arrow indicates the research area. c. The study area from western direction with  
4 tapes along profiles S4-S10 and with Danube River in the background. The profiles are closely West-East  
5 orientated. The dotted red line shows the main fracture which is directly visible from the opposite direction. The  
6 scarp is about 6m from the east end of the tapes. d. The main fracture from the east with profiles S4-10. The  
7 main crack branches off here. The area which had been cultivated is in the background. The long profile (P2)  
8 elongated between two vineyards in line S10.

9  
10 **Fig. 5** The measurement process; a. The instrument; b. Measurement and data registration; c. Plan of the Pre-P  
11 method; d. Exploration of the crack detected by the Pre-P method and removal of vegetation from the suspected  
12 crack location; e. A partially explored crack. There are often visible indications of cracks; f. Part of the crack  
13 which has been explored (No. II, see Figure 8 below).

14  
15 **Fig. 6** Profiles N6 and N8. MF: main fracture

16  
17 **Fig. 7** Profiles S6 and S8. MF: main fracture

18  
19 **Fig. 8** The Pre-P map. Solid yellow line marks the crack which is directly visible. Dashed yellow line: supposed  
20 cracks almost parallel to the scarp on the basis of the map. Dashed purple lines: supposed cracks almost  
21 perpendicular to the scarp on the basis of the Pre-P map. Dashed black lines marking the explored crack. Dotted  
22 black curve: partially excavated cracks. Arabic numerals indicate mechanically stable areas, Roman numbers the  
23 supposed cracks.

24  
25 **Fig. 9** Pre-P results on Profile 2 which extends the area studied in detail. The solid arrows indicate the position  
26 of the larger crack and the dotted arrows those of the smaller cracks. The solid rectangles indicate the rock zones  
27 in the passive area, the dotted rectangles in the active area. Black arrows show the effect of lanes caused by cars.  
28 MF: main fracture.

29  
30 **Fig. 10** The profiles which extended into the passive area. The dotted lines project the position of the anomalies  
31 to the horizontal axis. The continuous lines connect fractures observed on both profiles which are assumed to be  
32 the same. MF: main fracture.

Figure 1  
[Click here to download high resolution image](#)

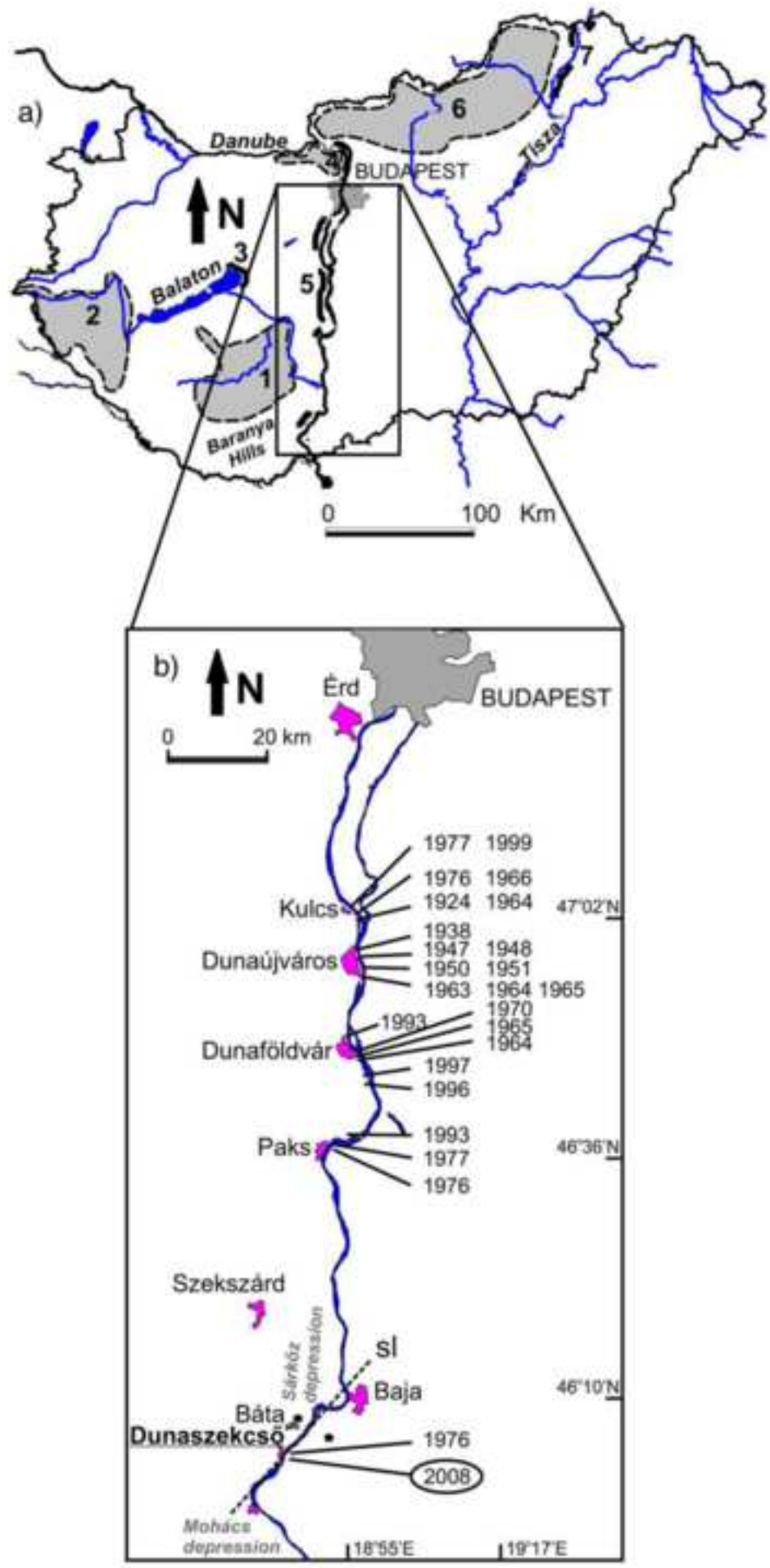


Figure 2  
[Click here to download high resolution image](#)

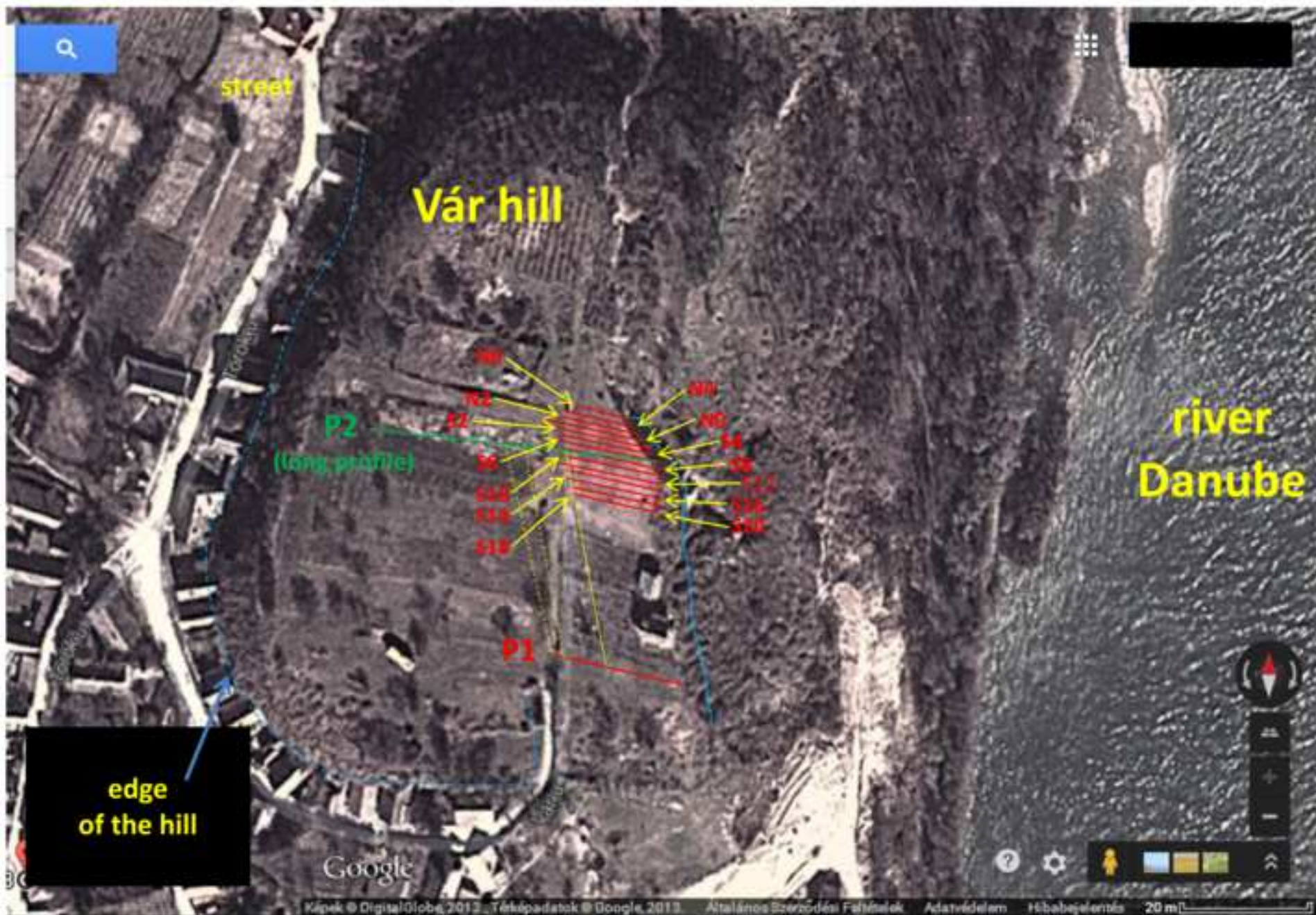


Figure 3  
[Click here to download high resolution image](#)

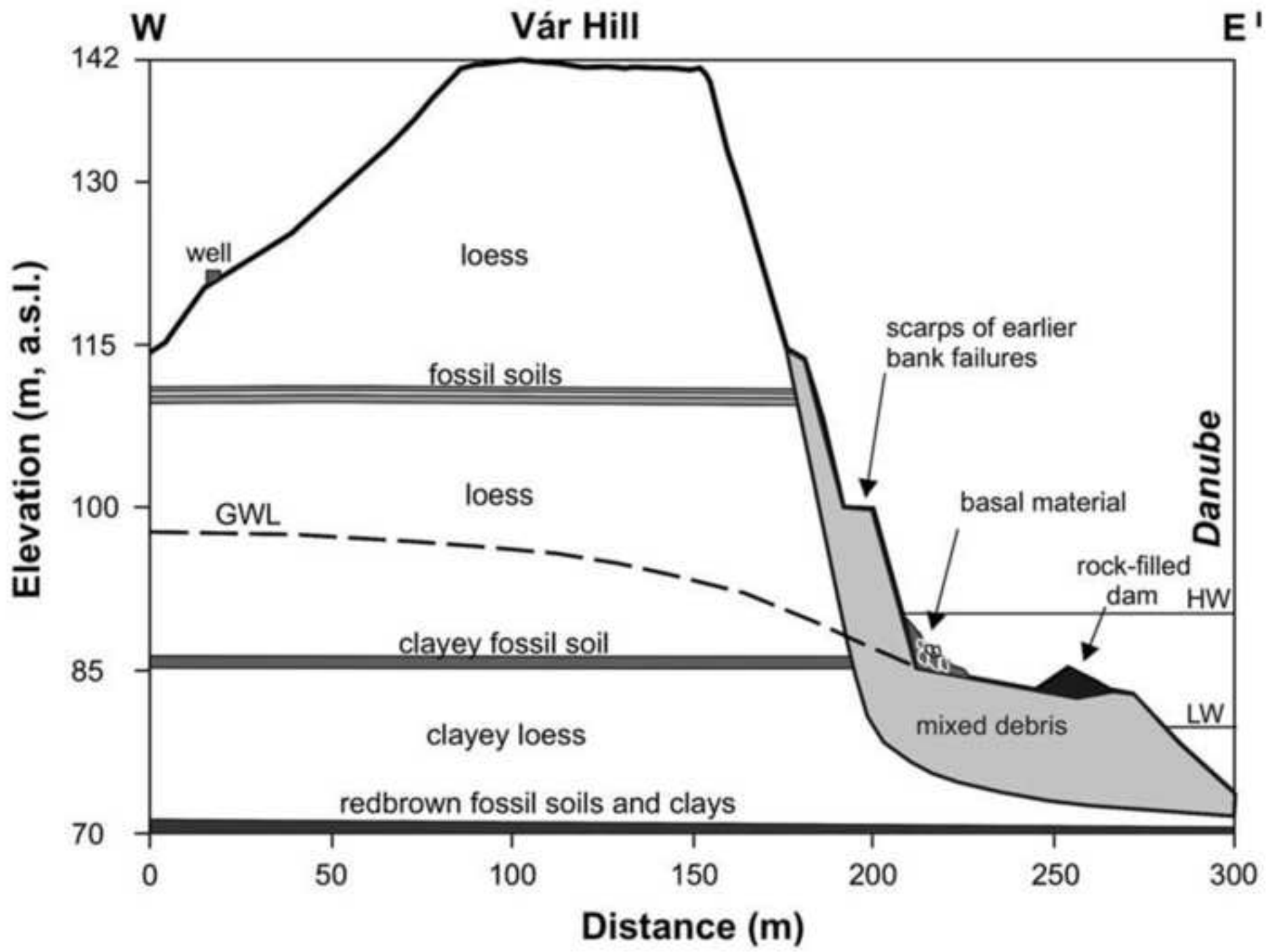




Figure 4  
[Click here to download high resolution image](#)



a.



b.



c.



d.

Figure 5  
[Click here to download high resolution image](#)

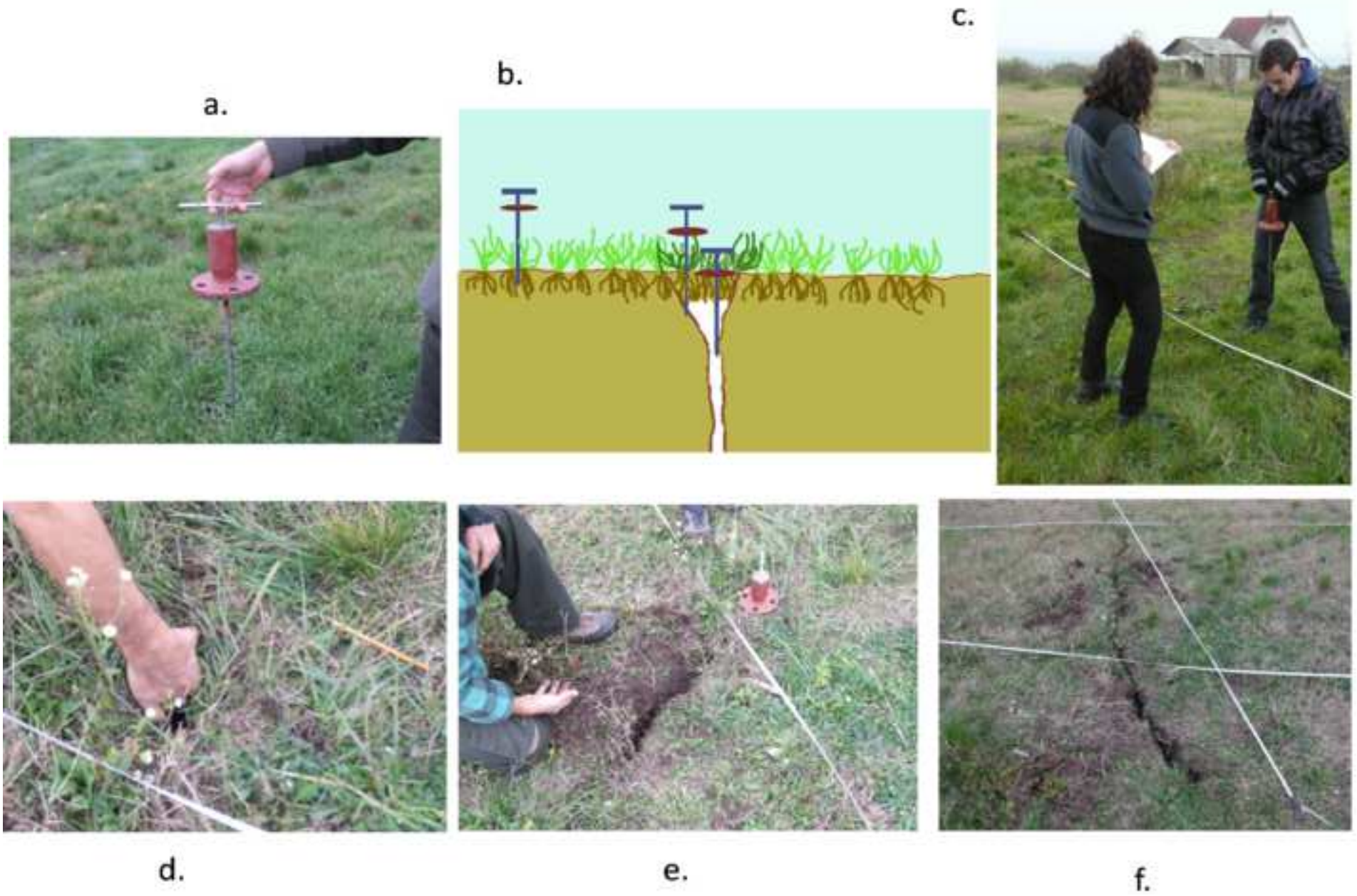


Figure 6  
[Click here to download high resolution image](#)

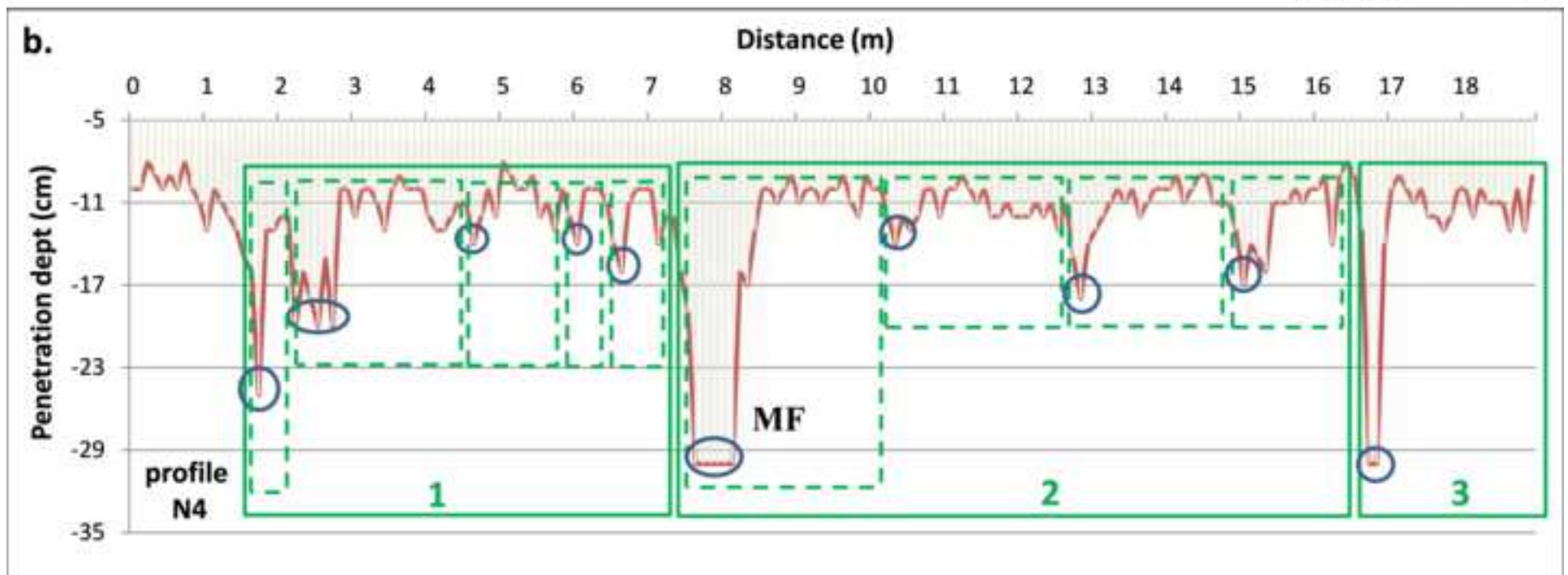
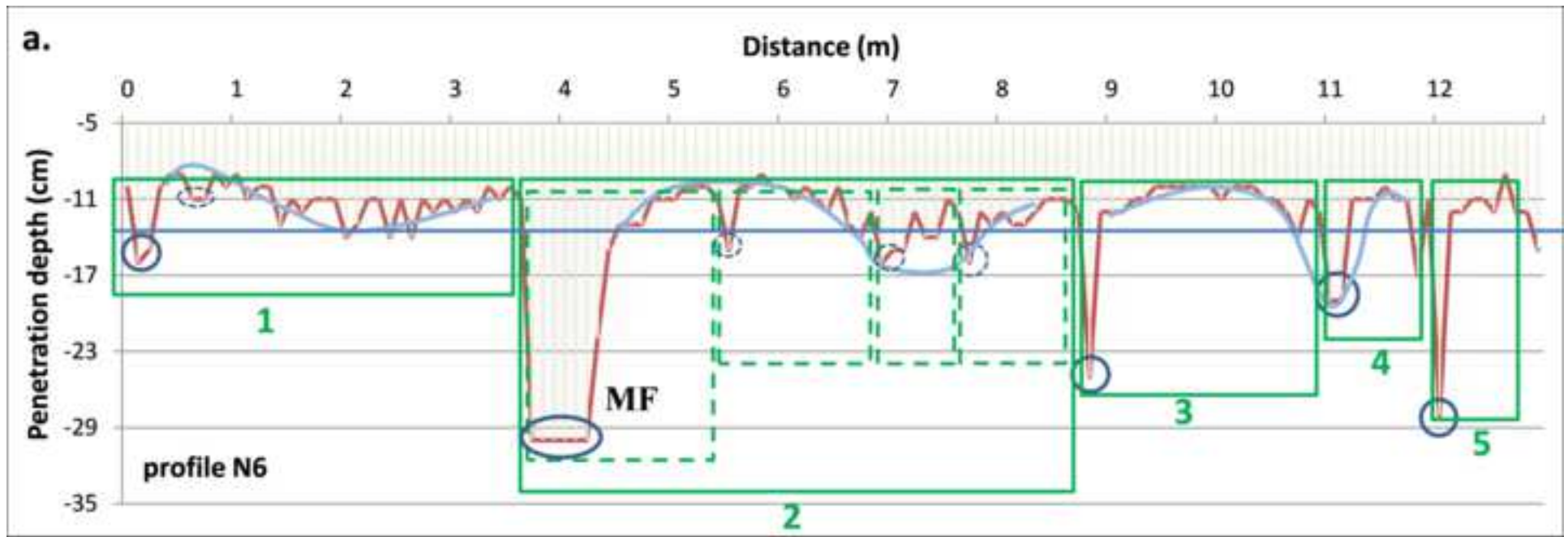


Figure 7  
[Click here to download high resolution image](#)

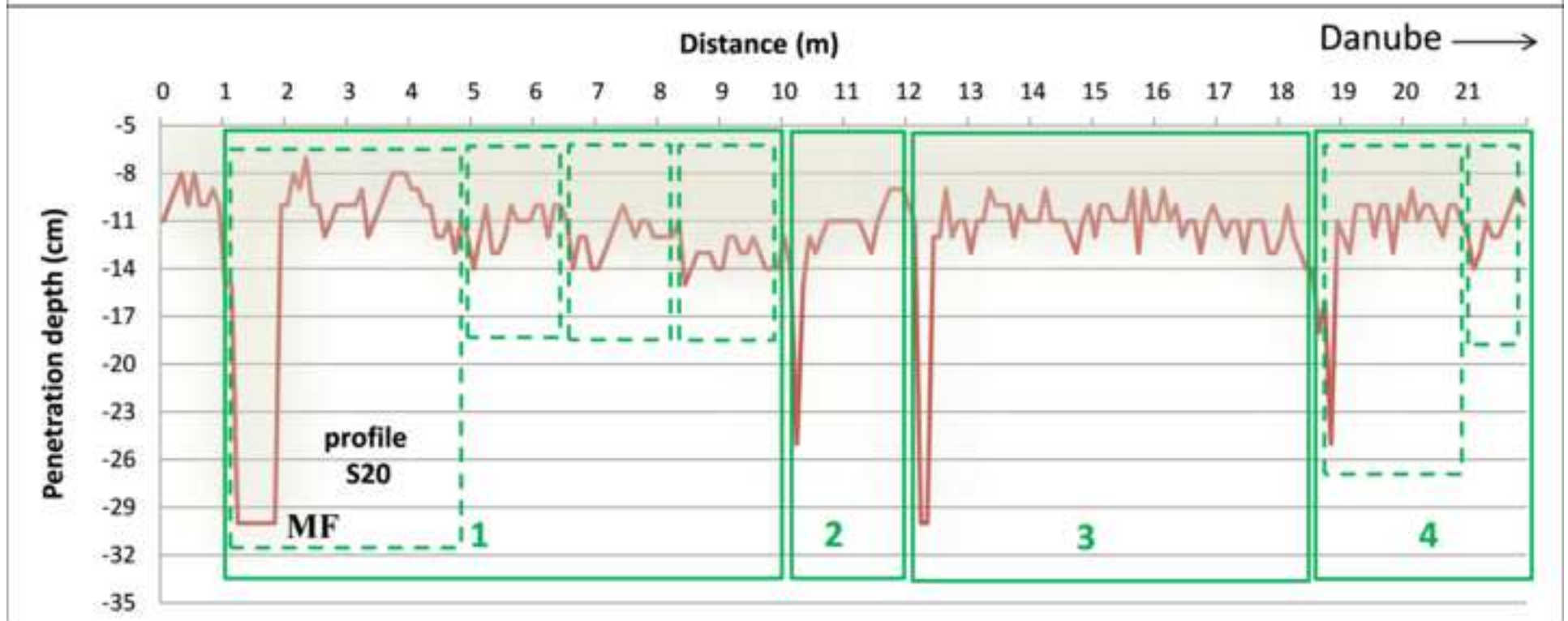
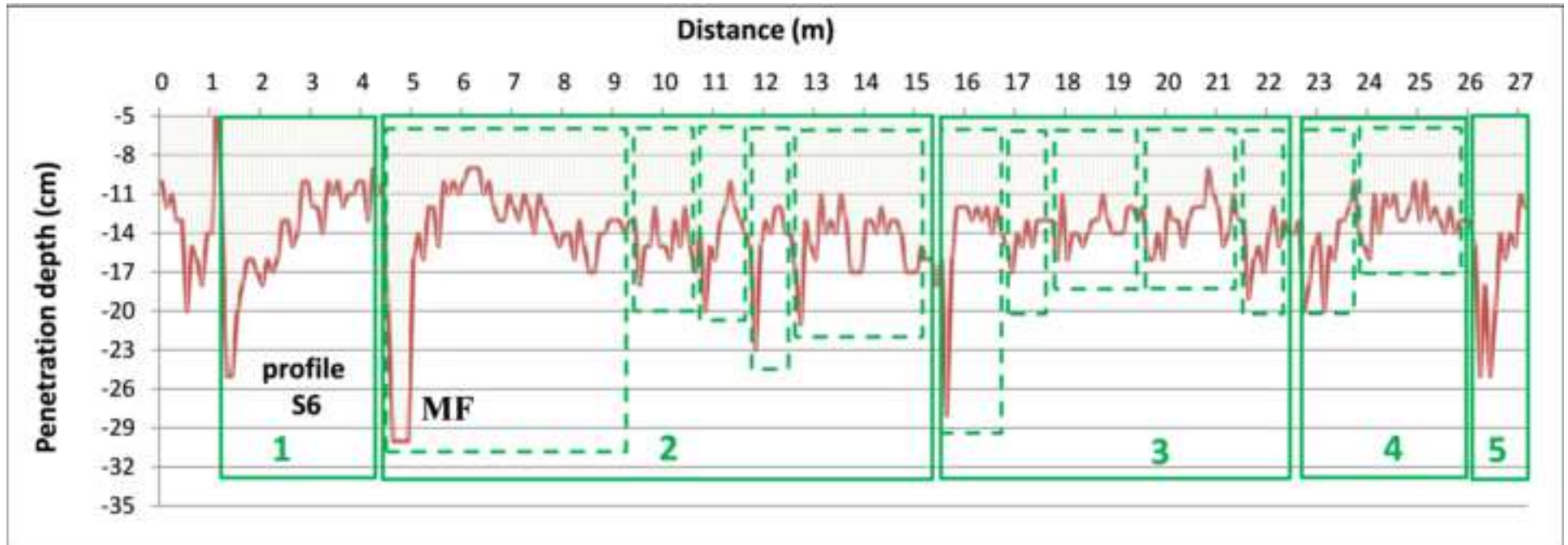


Figure 8  
[Click here to download high resolution image](#)

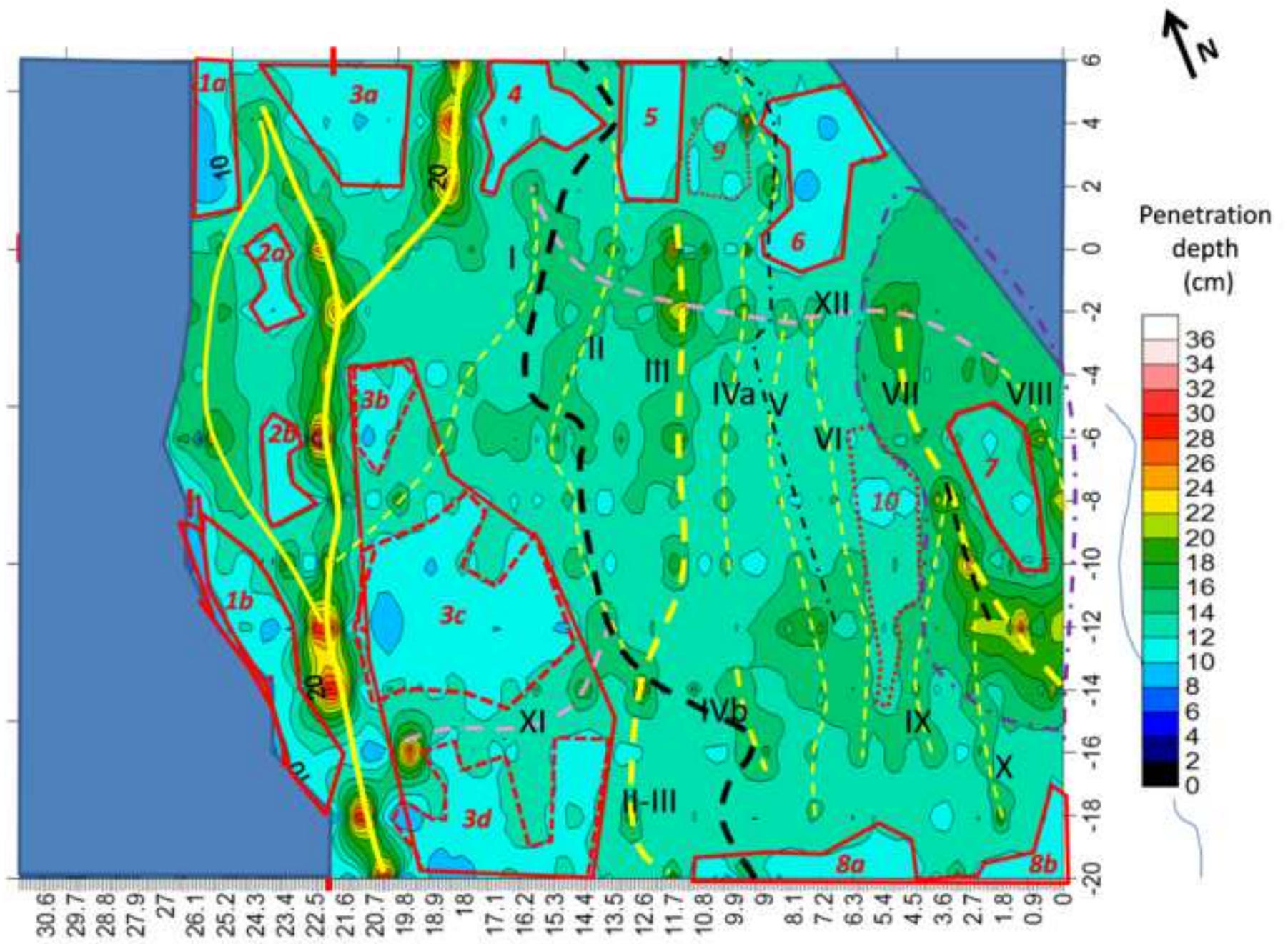


Figure 9  
[Click here to download high resolution image](#)

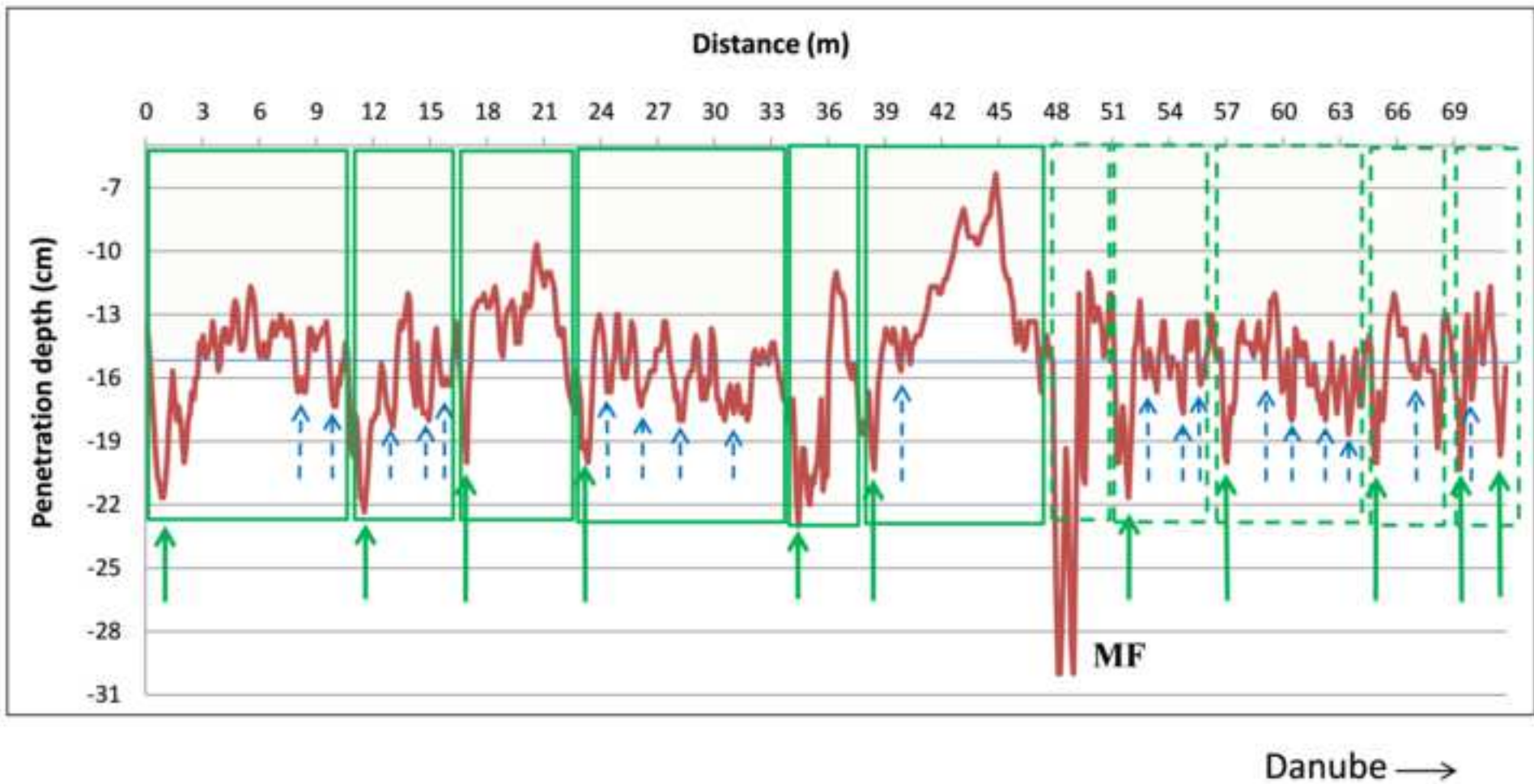


Figure 10  
[Click here to download high resolution image](#)



### Profile P1

